

An insight into the flux calibration of Gaia G-band images and BP/RP spectrophotometry

E. Pancino

INAF – Bologna Observatory, Via Ranzani 1, I-40127 Bologna, Italy

Abstract.

The Gaia mission is described, focussing on those technical aspects that are necessary to understand the details of its external (absolute) flux calibration. On board of Gaia there will be two (spectro)photometers, the blue one (BP) and the red one (RP) covering the range 330-1050 nm, and the white light (G-band) imager dedicated to astrometry. Given the fact that the focal plane of Gaia will be constituted by 105 CCDs and the sources will cross the the focal plane at constant speed, at different positions in each of the foreseen passages (on average 70–80, but up to 350) in the mission lifetime, the “simple” problem of calibrating the integrated BP/RP and G-band magnitudes and the low resolution BP/RP spectra flux turns into a very delicate and complicated issue, including CTI effects, LSF variations across the focal plane and with time, CCD gating to avoid saturation and the like. The calibration model requires a carefully selected set of $\simeq 200$ SpectroPhotometric Standard Stars (SPSS) with a nominal precision of a few %, with respect to Vega.

1. The Gaia mission

Gaia is a cornerstone mission of the ESA Space Program, presently scheduled for launch in 2012. The Gaia satellite will perform an all-sky survey to obtain parallaxes and proper motions to μas precision for about 10^9 point-like sources and astrophysical parameters (T_{eff} , $\log g$, $E(B - V)$, metallicity etc.) for stars down to a limiting magnitude of $V \simeq 20$, plus 2-30 km/s accuracy (depending on spectral type), radial velocities for several millions of stars down to $V < 17$.

Such an observational effort has been compared to the mapping of the human genome for the amount of collected data and for the impact that it will have on all branches of astronomy and astrophysics. The expected end-of-mission astrometric accuracies are almost 100 times better than the HIPPARCOS dataset (see Perryman et al. 1997). This exquisite precision will allow a full and detailed reconstruction of the 3D spatial structure and 3D velocity field of the Milky Way galaxy within $\simeq 10$ kpc from the Sun. This will provide answers to long-standing questions about the origin and evolution of our Galaxy, from a quantitative census of its stellar populations, to a detailed characterization of its substructures (as, for instance, tidal streams in the Halo, see Ibata & Gibson, 2007, *Sci. Am.*, 296, 40), to the distribution of dark matter.

The accurate 3D motion of more distant Galactic satellites (as globular clusters and the Magellanic Clouds) will be also obtained by averaging the proper motions of many thousands of member stars: this will provide an unprecedented leverage to constrain the mass distribution of the Galaxy and/or non-standard theories of gravitation. Gaia will determine direct geometric distances to essentially any kind of standard candle currently used for distance determination, setting the whole cosmological distance scale on extremely firm bases.

Table 1: Expected numbers of specific objects observed by Gaia.

Type	Numbers	Type	Numbers
Extragalactic supernovae	20 000	Extra-solar planets	15 000
Resolved galaxies	10^6 – 10^7	Disk white dwarfs	200 000
Quasars	500 000	Astrometric microlensing events	100
Solar system objects	250 000	Photometric microlensing events	1000
Brown dwarfs	≥ 50 000	Resolved binaries (within 250 pc)	10^7

As challenging as it is, the processing and analysis of the huge data-flow incoming from Gaia is the subject of thorough study and preparatory work by the Data Processing and Analysis Consortium (DPAC), in charge of all aspects of the Gaia data reduction. The consortium comprises more than 400 scientists from 25 European institutes. Gaia is usually described as a self-calibrating mission, but it also needs *external* data to fix the zero-point of the magnitude system and radial velocities, and to calibrate the classification/parametrization algorithms. *All these additional data are termed auxiliary data and have to be available, at least in part, three months before launch.* While part of the auxiliary data already exist and must only be compiled from archives, this is not true for several components. To this aim a coordinated programme of ground-based observations is being organized by a dedicated inter-CU committee (GBOG), that promotes synergies and avoids duplications of effort.

1.1. Science goals and capabilities

Gaia will measure the positions, distances, space motions, and many physical characteristics of some billion stars in our Galaxy and beyond. For many years, the state of the art in celestial cartography has been the Schmidt surveys of Palomar and ESO, and their digitized counterparts. The measurement precision, reaching a few millionths of a second of arc, will be unprecedented. Some millions of stars will be measured with a distance accuracy of better than 1 per cent; some 100 million or more to better than 10 per cent. Gaia’s resulting scientific harvest is of almost inconceivable extent and implication.

Gaia will provide detailed information on stellar evolution and star formation in our Galaxy. It will clarify the origin and formation history of our Galaxy. The results will precisely identify relics of tidally-disrupted accretion debris, probe the distribution of dark matter, establish the luminosity function for pre-main sequence stars, detect and categorize rapid evolutionary stellar phases, place unprecedented constraints on the age, internal structure and evolution of all stellar types, establish a rigorous distance scale framework throughout the Galaxy and beyond, and classify star formation and kinematical and dynamical behaviour within the Local Group of galaxies.

Gaia will pinpoint exotic objects in colossal and almost unimaginable numbers: many thousands of extra-solar planets will be discovered (from both their astrometric wobble and from photometric transits) and their detailed orbits and masses determined; tens of thousands of brown dwarfs and white dwarfs will be identified; tens of thousands of extragalactic supernovae will be discovered; Solar System studies will receive a massive impetus through the observation of hundreds of thousands of minor planets; near-Earth objects, inner Trojans and even new trans-Neptunian objects, including Plutinos, may be discovered.

Gaia will follow the bending of star light by the Sun and major planets over the entire celestial sphere, and therefore directly observe the structure of space-time – the accuracy of its measurement of General Relativistic light bending may reveal the long-sought scalar correction to its tensor form. The PPN parameters γ and β , and the solar quadrupole

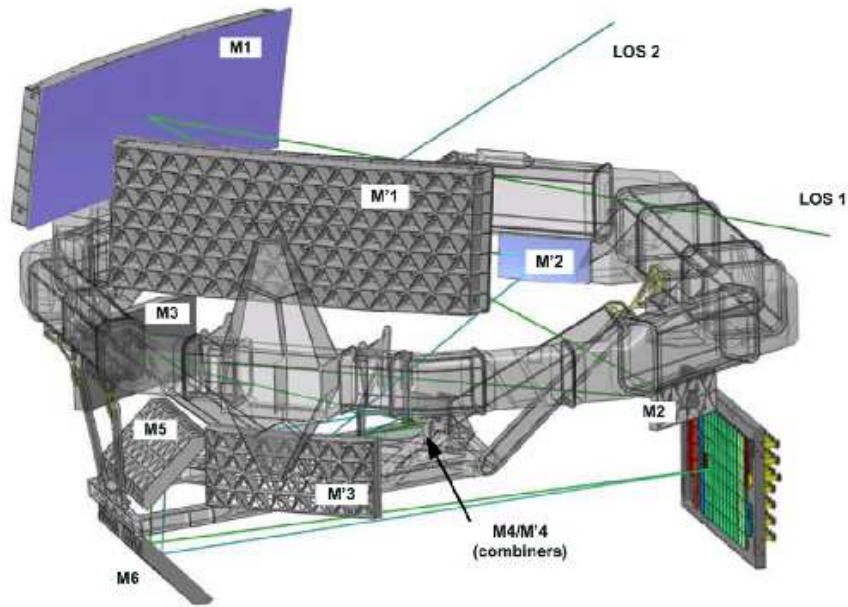


Figure 1: The two Gaia telescopes, mounted on a compact torus, point towards two lines of sight separated by 106.5° , and converging on the same focal plane. ©ESA

moment J2, will be determined with unprecedented precision. All this, and more, through the accurate measurement of star positions.

We summarize some of the most interesting object classes that will be observed by Gaia, with estimates of the expected total number of objects, in Table 1. For more information on the Gaia mission: <http://www.rssd.esa.int/Gaia>. More information for the public on Gaia and its science capabilities are contained in the *Gaia information sheets*¹. An excellent review of the science possibilities opened by Gaia can be found in Perryman et al. (1997).

1.2. Launch, timeline and data releases

The first idea for Gaia began circulating in the early 1990, culminating in a proposal for a cornerstone mission within ESA's science programme submitted in 1993, and a workshop in Cambridge in June 1995. By the time the final catalogue will be released approximately in 2020, almost two decades of work will have elapsed between the original concept and mission completion.

Gaia will be launched by a Soyuz carrier (rather than the initially foreseen Ariane 5) in 2012 from French Guyana and will start operating once it will reach its Lissajous orbit around L2 (the unstable Lagrange point of the Sun and Earth-Moon system), in about one month. Two ground stations will receive the compressed Gaia data during the 5 years² of operation: Cebreros (Spain) and Perth (Australia). The data will then be transmitted to the main data centers throughout Europe to allow for data processing. We are presently in technical development phase C/D, and the hardware is being built, tested and assembled. Software development started in 2006 and is presently producing and testing pipelines with

¹http://www.rssd.esa.int/index.php?project=GAIA&page=Info_sheets_overview.

²If – after careful evaluation – the scientific output of the mission will benefit from an extension of the operation period, the satellite should be able to gather data for one more year, remaining within the Earth eclipse.

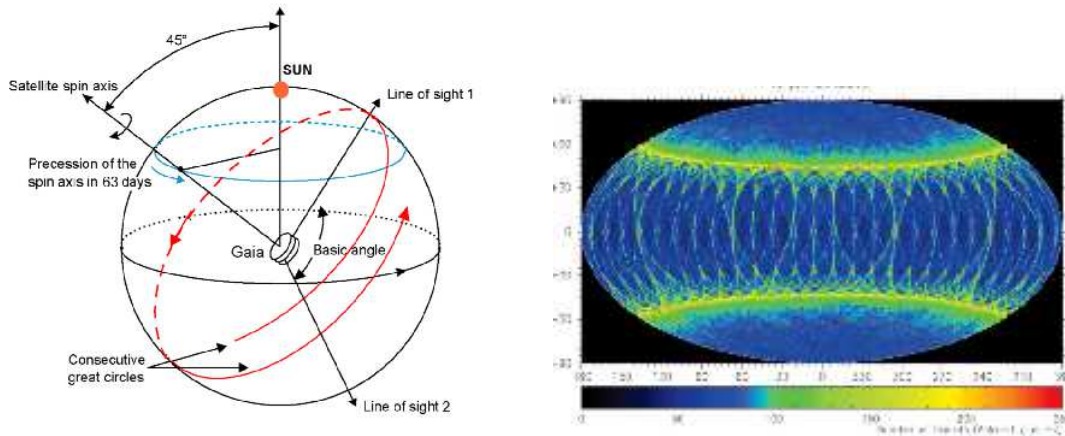


Figure 2: Left: the scanning law of Gaia during main operations; Right: the average number of passages on the sky, in ecliptic coordinates. ©ESA

the aim of delivering to the astrophysical community a full catalogue and dataset ready for scientific investigation.

Apart from the end-of-mission data release, foreseen around 2020, some intermediate data releases are foreseen. In particular, there should be one first intermediate release covering either the first 6 months or the first year of operation, followed by a second and possibly a third intermediate release, that are presently being discussed. The data analysis will proceed in parallel with observations, the major pipelines re-processing all the data every 6 months, with secondary cycle pipelines – dedicated to specific tasks – operating on different timescales. In particular, verified science alerts, based on unexpected variability in flux and/or radial velocity, are expected to be released within 24 hours from detection, after an initial period of testing and fine-tuning of the detection algorithms.

1.3. Mission concepts

During its 5-year operational lifetime, the satellite will continuously spin around its axis, with a constant speed of 60 arcsec/sec. As a result, over a period of 6 hours, the two astrometric fields of view will scan across all objects located along the great circle perpendicular to the spin axis (Figure 2, left panel). As a result of the basic angle of 106.5° separating the astrometric fields of view on the sky (Figure 1), objects transit the second field of view with a delay of 106.5 minutes compared to the first field. Gaia’s spin axis does not point to a fixed direction in space, but is carefully controlled so as to precess slowly on the sky. As a result, the great circle that is mapped by the two fields of view every 6 hours changes slowly with time, allowing repeated full sky coverage over the mission lifetime. The best strategy, dictated by thermal stability and power requirements, is to let the spin axis precess (with a period of 63 days) around the solar direction with a fixed angle of 45° . The above scanning strategy, referred to as “revolving scanning”, was successfully adopted during the Hipparcos mission.

Every sky region will be scanned on average 70-80 times, with regions lying at $\pm 45^\circ$ from the Ecliptic Poles being scanned on average more often than other locations. Each of the Gaia targets will be therefore scanned (within differently inclined great circles) from a minimum of approximately 10 times to a maximum of 250 times (Figure 2, right panel). Only point-like sources will be observed, and in some regions of the sky, like the Baade’s window, ω Centauri or other globular clusters, the star density of the two combined fields of view will be of the order of 750 000 or more per square degree, exceeding the storage capability of the onboard processors, so Gaia will not study in detail these dense areas.

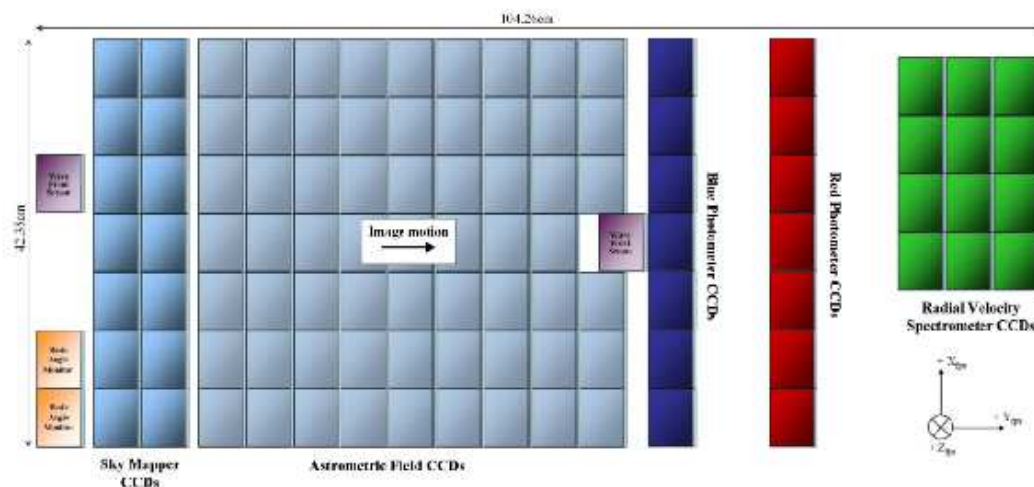


Figure 3: The 105 on the Gaia focal plane. ©ESA

1.4. Focal plane

Figure 3 shows the focal plane of Gaia, with its 105 CCDs, which are read in TDI (Time Delay Integration) mode: objects enter the focal plane from the left and cross one CCD in 4 seconds. Apart from some technical CCDs that are of little interest in this context, the first two CCD columns, the Sky Mappers (SM), perform the on-board detection of point-like sources, each of the two columns being able to see only one of the two lines of sight. After the objects are identified and selected, small windows are assigned, which follow them in the astrometric field (AF) CCDs where white light (or G-band) images are obtained (Section 1.5.). Immediately following the AF, two additional columns of CCDs gather light from two slitless prism spectrographs, the blue spectrophotometer (BP) and the red one (RP), which produce dispersed images (Section 1.6.). Finally, objects transit on the Radial Velocity Spectrometer (RVS) CCDs to produce higher resolution spectra around the Calcium Triplet (CaT) region (Section 1.7.).

1.5. Astrometry

The AF CCDs will provide G-band images, i.e., white light images where the passband is defined by the telescope optics transmission and the CCDs sensitivity, with a very broad combined passband ranging from 330 to 1050 nm and peaking around 500–600 nm (Figure 4). The objective of Gaia’s astrometric data reduction system is the construction of core mission products: the five standard astrometric parameters, position (α , δ), parallax (ϖ), and proper motion (μ_α , μ_δ) for all observed stellar objects. The expected end-of-mission precision in the proper motions is expected to be better than $10 \mu\text{as}$ for $G < 10$ stars, $25 \mu\text{as}$ for $G = 15$, and $300 \mu\text{as}$ for $G = 20$. For parallaxes, considering a $G = 12$ star, we can expect to have distances at better than 0.1% within 250 pc, 1% within 2700 pc, and 10% within 10 kpc.

To reach these end-of-mission precisions, the average 70–80 observations per target gathered during the 5-year mission duration will have to be combined into a single, global, and self-consistent manner. 40 Gb of telemetry data will first pass through the Initial Data Treatment (IDT) which determines the image parameters and centroids, and then performs an object cross-matching. The output forms the so-called One Day Astrometric Solution (ODAS), together with the satellite attitude and calibration, to the sub-milliarcsecond accuracy. The data are then written to the Main Database.

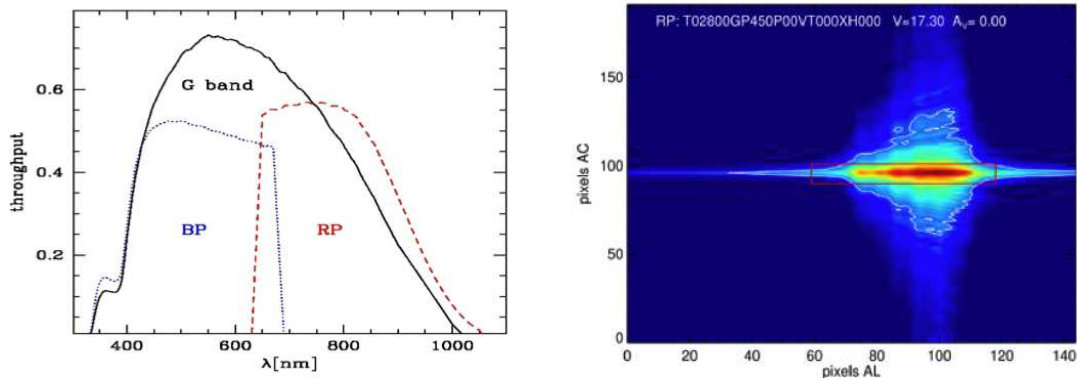


Figure 4: Left: the passbands of the G-band, BP and RP; Right: a simulated RP dispersed image, with a red rectangle marking the window assigned for compression and ground telemetry. ©ESA

The next step is the Astrometric Global Iterative Solution (AGIS) processing. AGIS processes together the attitude and calibration parameters with the source parameters, refining them in an iterative procedure that stops when the adjustments become sufficiently small. As soon as new data come in, on the basis of 6 months cycles, all the data in hand are reprocessed together from scratch. This is the only scheme that allows for the quoted precisions, and it is also the philosophy that justifies Gaia as a self-calibrating mission. The primary AGIS cycle will treat only stars that are flagged as single and non-variable (expected to be around 500 millions), while other kinds of objects will be computed in secondary AGIS cycles that utilize the main AGIS solution. Dedicated pipelines for specific kinds of objects (asteroids, slightly extended objects, variable objects and so on) are being put in place to extract the best possible precision. Owing to the large data volume (100 Tb) that Gaia will produce, and to the iterative nature of the processing, the computing challenges are formidable: AGIS processing alone requires some 10^{21} FLOPs which translates to runtimes of months on the ESAC computers in Madrid.

1.6. Spectrophotometry

The primary aim of the photometric instrument is mission critical in two respects: (i) to correct the measured centroids position in the AF for systematic chromatic effects, and (ii) to classify and determine astrophysical characteristics of all objects, such as temperature, gravity, mass, age and chemical composition (in the case of stars).

The BP and RP spectrophotometers are based on a dispersive-prism approach such that the incoming light is not focussed in a PSF-like spot, but dispersed along the scan direction in a low-resolution spectrum. The BP operates between 330–680 nm while the RP between 640–1000 nm (Figure 4). Both prisms have appropriate broad-band filters to block unwanted light. The two dedicated CCD stripes cover the full height of the AF and, therefore, all objects that are imaged in the AF are also imaged in the BP and RP.

The resolution is a function of wavelength, ranging from 4 to 32 nm/pix for BP and 7 to 15 nm/pix for RP. The spectral resolution, $R=\lambda/\delta\lambda$ ranges from 20 to 100 approximately. The dispersers have been designed in such a way that BP and RP spectra are of similar sizes (45 pixels). Window extensions meant to measure the sky background are implemented. To compress the amount of data transmitted to the ground, all the BP and RP spectra – except for the brightest stars – are binned on chip in the across-scan direction, and are transmitted to the ground as one-dimensional spectra. Figure 4 shows a simulated RP spectrum, unbinned, before windowing, compression, and telemetry.

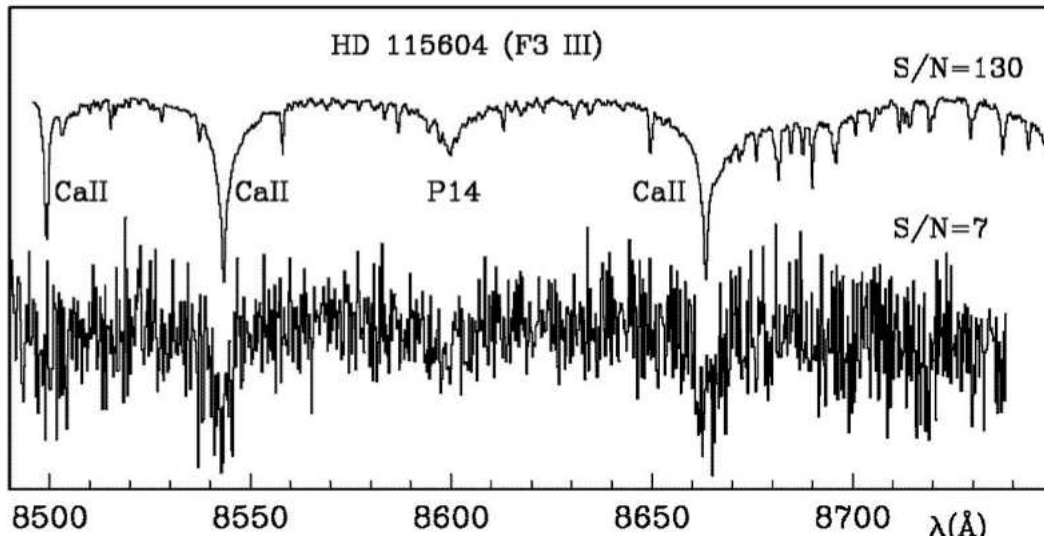


Figure 5: Simulated RVS end-of-mission spectra for the extreme cases of 1 single transit (bottom spectrum) and of 350 transits (top spectrum). ©ESA

The final data products will be the end-of-mission (or intermediate releases) of global, combined BP and RP spectra and integrated magnitudes M_{BP} and M_{RP} . Epoch spectra will be released only for specific classes of objects, such as variable stars and quasars, for example. The internal flux calibration of integrated magnitudes, including the M_G magnitudes as well, is expected at a precision of 0.003 mag for $G=13$ stars, and for $G=20$ stars goes down to 0.07 mag in M_G , 0.3 mag in M_{BP} and M_{RP} . The external calibration should be performed with a precision of the order of a few percent (with respect to Vega).

1.7. High-resolution spectroscopy

The primary objective of the RVS is the acquisition of radial velocities, which combined with positions, proper motions, and parallaxes will provide the means to decipher the kinematical state and dynamical history of our Galaxy.

The RVS will provide the radial velocities of about 100–150 million stars up to 17-th magnitude with precisions ranging from 15 km s^{-1} at the faint end, to 1 km s^{-1} or better at the bright end. The spectral resolution, $R=\lambda/\delta\lambda$ will be 11 500. Radial velocities will be obtained by cross-correlating observed spectra with either a template or a mask. An initial estimate of the source atmospheric parameters will be used to select the most appropriate template or mask. On average, 40 transits will be collected for each object during the 5-year lifetime of Gaia, since the RVS does not cover the whole width of the Gaia AF (Figure 3). In total, we expect to obtain some 5 billion spectra (single transit) for the brightest stars. The analysis of this huge dataset will be complicated, not only because of the sheer data volume, but also because the spectroscopic data analysis relies on the multi-epoch astrometric and photometric data.

The covered wavelength range (847–874 nm) (Figure 5) is a rich domain, centered on the infrared calcium triplet: it will not only provide radial velocities, but also many stellar and interstellar diagnostics. It has been selected to coincide with the energy distribution peaks of G and K type stars, which are the most abundant targets. In early type stars, RVS spectra may contain also weak Helium lines and N, although they will be dominated by the Paschen lines. The RVS data will effectively complement the astrometric and photometric observations, improving object classification. For stellar objects, it will provide atmospheric parameters such as effective temperature, surface gravity, and individual abundances of key

elements such as Fe, Ca, Mg, Si for millions of stars down to $G \simeq 12$. Also, Diffuse Intertellar Bands (DIB) around 862 nm will enable the derivation of a 3D map of interstellar reddening.

1.8. The DPAC

ESA will take care of the satellite design, build and testing phases, of launch and operation, and of the data telemetry to the ground, managing the ESAC datacenter in Madrid, Spain. The data treatment and analysis is instead responsibility of the European scientific community. In 2006, the announcement of opportunity opened by ESA was successfully answered by the Data Processing and Analysis Consortium (DPAC), a consortium that is presently counting more than 400 scientists in Europe (and outside) and more than 25 scientific institutions.

The DPAC governing body, or executive (DPACE) oversees the DPAC activities and the work has been organized among a few Coordination Units (CU) in charge of different aspects of data treatment:

- **CU1. System Architecture** (manager: O' Mullane), dealing with all aspects of hardware and software, and coordinating the framework for software development and data management.
- **CU2. Data Simulations** (manager: Luri), in charge of the simulators of various stages of data products, necessary for software development and testing.
- **CU3. Core processing** (manager: Bastian), developing the main pipelines such as IDT, AGIS and astrometry processing in general.
- **CU4. Object Processing** (managers: Pourbaix/Tanga), for the processing of objects that require special treatment such as minor bodies of the Solar system, for example.
- **CU5. Photometric processing** (manager: van Leeuwen), dedicated to the BP, RP, and M_G processing and calibration, including image reconstruction, background treatment, and crowding treatment, among others.
- **CU6. Spectroscopic Processing** (managers: Katz/Cropper), dedicated to RVS processing and radial velocity determination.
- **CU7. Variability Processing** (managers: Eyer/Evans/Dubath), dedicated to processing, classification and parametrization of variable objects.
- **CU8. Astrophysical Parameters** (managers: Bailer-Jones/Thevenin), developing object classification software and, for each object class, software for the determination of astrophysical parameters.
- **CU9. Catalogue Production and Access** (to be activated in the near future), responsible for the production of astrophysical catalogues and for the publication of Gaia data to the scientific community.

These are flanked by a few working groups (WG) that deal with aspects that are either transversal among the various CUs (such as the GBOG, coordinating the ground based observations for the external calibration of Gaia) or of general interest (such as the Radiation task force, serving as the interface between DPAC and the industry in all matters related to CCD radiation tests).

2. The flux calibration of Gaia data

Calibrating (spectro)photometry obtained from the usual type of ground based observations (broadband imaging, spectroscopy) is not a trivial task, but the procedures are well known (see e.g., Bessell, 1999) and several scientists have developed sets of standard stars appropriated for the more than 200 photometric systems known, and for spectroscopic observations. Generally, magnitudes are calibrated to a standard system with equations in the form

$$M = m + ZP + \alpha(\text{colour}) + \beta(\text{airmass})$$

where M is the calibrated magnitude in a chosen photometric band, m the observed (instrumental) one in the same (or very similar) band, α is the colour term and β the extinction coefficient, due the Earth atmospheric extinction. For the spectra, usually the instrumental effect on the observed spectral energy distribution (SED) is parametrized as

$$S_{obs}(\lambda) = R(\lambda) S(\lambda)$$

where the observed SED, $S_{obs}(\lambda)$, is the result of the convolution of the “true” SED, $S(\lambda)$, with all the instrumental (transmissivity, quantum efficiencies) effects, which are empirically determined in the form of a response curve $R(\lambda)$ through the use of spectrophotometric standard stars (SPSS). In the case of Gaia, several instrumental effects – much more complex than those usually encountered – redistribute light along the SED of the observed objects. In particular: the TDI integration mode, the fact that the focal plane is so large, the radiation damage and resulting CTI (charge transfer inefficiencies), the fact that the whole instrumental model is well known only before launch.

2.1. Challenges

The most difficult Gaia data to calibrate are the BP and RP spectra, requiring a new approach to the derivation of the calibration model (Section 2.3.) and to the SPSS needed to perform the actual calibration (Section 3.). The large focal plane with its large number of CCDs makes it so that different observations of the same star will be generally on different CCDs, with different quantum efficiencies. Also, each CCD is in a different position, with different optical distortions, optics transmissivity and so on. Therefore, each wavelength and each position across the focal plane has its (sometimes very different) PSF (point spread function). The TDI and continuous reading mode, combined with the need of compressing the data before on-ground transmission, make it necessary to translate the full PSF into a linear (compressed into 1D) LSF (line spread function), which of course add complication into the picture. In-flight instrument monitoring is foreseen, but never comparable to the full characterization that will be performed before launch, so the real instrument – at a certain observation time – will be different from the theoretical one assumed initially, and this difference will change with time.

Special mention deserves the radiation damage, one of the most important factors in the time variation of the instrument model. It has particular impact onto the BP and RP dispersed images since the objects travel along the BP and RP CCD strips in a direction that is parallel to the spectral dispersion (wavelength coordinate). Radiation damage causes traps that subtract photons from each passing object at a position corresponding to a certain wavelength. Slow traps release the trapped charges once the object is already passed, while fast traps can release the charges within the same object, but at a different wavelength. Given the low resolution, one pixel can cover as much as 15–20 nm (depending on the wavelength) and therefore the net effect of radiation damage can be to alter significantly the SED of some spectra. Possible solutions under testing are the equivalent of CCD pre-flashing, the statistical modeling of the traps behaviour and the fact that different transits for the same object will be affected differently by CTI effects, allowing for a certain degree of correction through average or median spectra. Finally the PSF/LSF itself is generally

larger than one Gaia pixel in the BP/RP spectra, introducing a large LSF smearing effect, i.e., the spread of photons with one particular wavelength into a large range of wavelengths.

In this paper, we will adopt the current Gaia calibration philosophy, where most of these instrumental effects are taken into account during the so-called internal flux calibration. A large number of well behaved stars (*internal standards*) observed by Gaia will be used to report all observations to a *reference* instrument, on the same instrumental flux and wavelength scales. All transits for each object observed by Gaia will be then averaged to produce one single BP and RP spectrum for each object, with its integrated instrumental magnitudes: M_G , M_{BP} , and M_{RP} . Only for specific classes of objects, epoch spectra and magnitudes will be released, with variable stars as an obvious example. The mean and epoch spectra will be mostly free from many of the problems examined just above, but they will still contain residuals due to the imperfect knowledge of the real instrument at each precise moment of time, and the most significant effects are expected to be the LSF smearing and the CTI effects.

In this paradigm, the internal and external flux and wavelength calibrations are treated as two entirely separated and consecutive pieces of the CU5 photometric pipeline, with different calibration models. So, from next Section, we start always from internally calibrated BP/RP spectra and M_G , M_{BP} , and M_{RP} magnitudes, without giving importance to the exact way they are produced. Presently, two alternative approaches are being considered to maximize the precision of the global calibration procedure: the first one is a *hybrid model* that partially combines internal and external models (Montegriffo et al. 2010), while the second is the so-called *full forwarding model* (Carrasco et al. 2010, in preparation), using the same calibration model for both the internal and external calibration.

2.2. The external calibration teams

Two Development units (DU) within CU5 (Photometric processing), are dedicated to the external calibration of Gaia photometry. They are DU13: “Instrument absolute response characterisation: ground-based preparation” coordinated by E. Pancino and DU14” “Instrument absolute response characterisation: definition and application” coordinated by C. Cacciari. They are both based in Bologna, Italy, in collaboration with the Bologna, Barcelona, and Groningen Universities. The actual team members at the time of writing are: G. Altavilla, M. Bellazzini, A. Bragaglia, C. Cacciari, J. M. Carrasco, G. Cocozza, L. Federici, F. Figueras, F. Fusi Pecci, C. Jordi, S. Marinoni, P. Montegriffo, E. Pancino, S. Ragaini, E. Rossetti, S. Trager.

2.3. Dispersion Matrix basic definition

If we concentrate now on the mean, internally calibrated BP/RP spectra calibration, we can write:

$$S_{obs}(\kappa_I) = \sum_{\lambda_i=0}^N T(\lambda_i) L_{\lambda_i}(\kappa_I - \kappa_P(\lambda_i)) S_{true}(\lambda_i)$$

where S_{obs} and S_{true} are the observed and “true” SEDs respectively, expressed the first in Gaia pixels κ_I and the second in wavelength intervals λ_i corresponding to the actual sampling of the SPSS used in the flux calibration process. $T(\lambda_i)$ is a combination of all the instrument and telescope transmissivity functions and aperture, while L is the LSF at a certain λ_i , centered at the appropriate κ_I pixel, but of course calculated over the whole wavelength interval from $\lambda_i=0$ to N (the total number of samples in the tabulated SPSS spectrum).

Such an equation can be written in its much simpler matricial form:

$$S_{obs} = D \times S_{true}$$

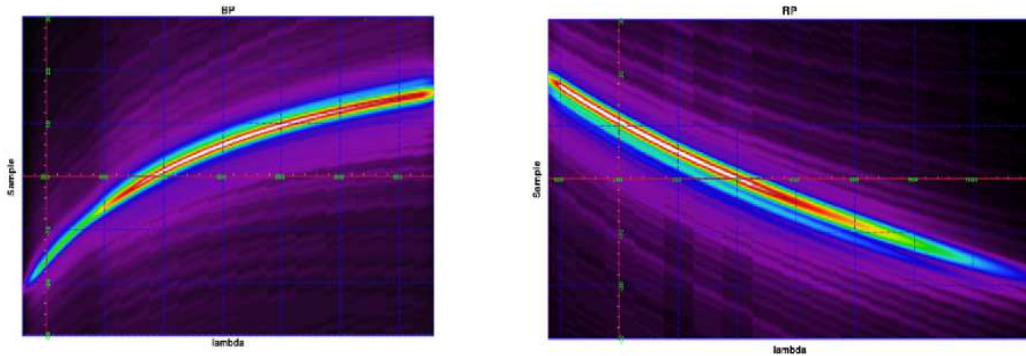


Figure 6: Graphical example of a dispersion matrix D , derived with a simulated SPSS set for the BP (left) and RP (right) instruments, on an arbitrary color scale. ©ESA

where D is called a “Dispersion Matrix”, an object that can be determined if S_{obs} and S_{true} are known, i.e., using a well defined set of SPSS observed by Gaia, that also have well known SED (see below). Once D is properly determined, it can be inverted to convert each mean, internally calibrated BP/RP spectrum³ (S_{obs}) into an flux calibrated spectrum S_{true}

$$S_{true} = D^{-1} \times S_{obs}$$

The main advantage of this approach is that D contains (and therefore corrects empirically for) the actual effects of LSF smearing – even if the real shape of the LSF is not perfectly known a priori. More than that, the effective LSF – as determined with the chosen SPSS set – at each wavelength can be extracted from each column of the matrix. The matrix rows represent instead the effective passbands corresponding to each Gaia pixel, including the full effect of LSF smearing. This peculiar property of the dispersion matrix makes it the best (and possibly only) solution to the external calibration of Gaia BP/RP spectra. By definition, the dispersion matrix D contains also the actual dispersion function, which can be seen in Figure 6 as the curved structure close to the diagonal of the matrix.

Finally, an important by-product of the described calibration model is the absolute wavelength calibration of the BP/RP spectra to a precision of *at least* a few tenths of a Gaia pixel⁴ (Montegriffo & Bellazzini 2009b), which is automatically performed together with the absolute flux calibration.

There are a few problems in the use of the dispersion matrix as proposed. We will discuss in the three following Sections the two most important ones and their proposed solutions: (1) the matrix is rectangular and its inversion is not so straightforward; (2) the matrix needs a set of independent vectors to be determined in a non-degenerate way (which also implies that the set of SPSS must be carefully chosen).

2.4. Smoothing the input SPSS spectra

Clearly, the dispersion matrix is a rectangular matrix: the Gaia observations have a smaller number of samples (pixels) than the SPSS spectra used to build their calibration model (wavelength sampling). Inverting a rectangular matrix is a non-trivial task so if we want

³Incidentally, for some object classes that need it, such as variable stars, sigle transits – the so called *epoch spectra* – will be published. The described calibration model can be applied also to single epoch spectra once they have been internally calibrated, i.e., reported to a common, instrumental scale of flux and wavelength.

⁴This first estimate of the wavelength zero point and scale precision is based on a slightly outdated calibration model formulation, an therefore has to be considered just as an upper limit to a more realistic uncertainty (Montegriffo, 2010, private communication).

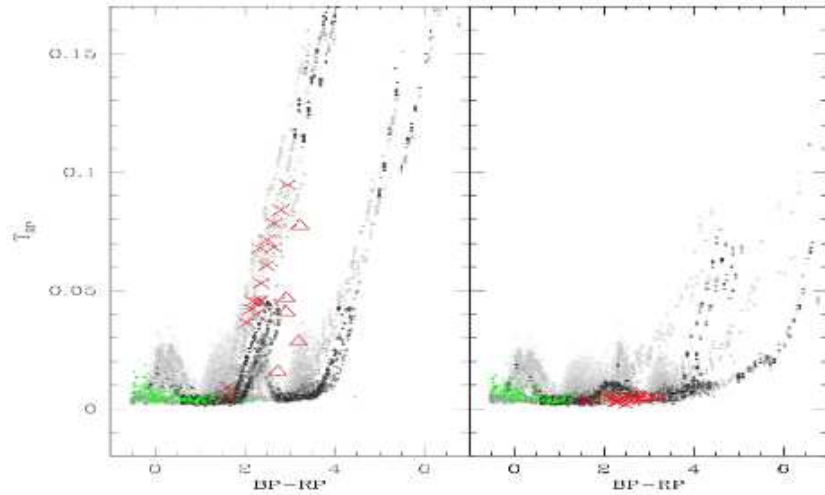


Figure 7: On both panels, grey dots are simulated spectra of different metallicity and reddening (this explains the parallel sequences). Green dots are white dwarfs and hot subdwarfs, while red symbols are different types of red stars with significant absorption features, i.e., molecular bands. Abscissae represent the BP–RP color, ordinates are the difference between the “known” magnitude of the used SEDs and the “calibrated” ones obtained with a dispersion matrix. Left: all points are calibrated with a matrix built only with hot spectral types (green dots): the reddest stars are calibrated with an *error* of 0.15 mag and more. Right: all points are calibrated with a matrix determined using also 10 red SPSS with absorption features (red symbols): all stars with SEDs similar to the 10 red stars ($2 \text{ mag} < \text{BP-RP} < 4 \text{ mag}$) are calibrated with an *error* of less than 1%. ©ESA

to use the inverted matrix to calibrate our data we must find a method to reduce the dimensionality of the input SPSS flux tables. A few different methods have been considered such as the B splines representation (Montegriffo & Bellazzini, 2009a), Gaussian smoothing with variable width Gaussians (Montegriffo, 2010, private communication), and smoothing through rectangular functions corresponding to the Gaia pixels (Montegriffo et al. 2010). The idea is that the S_{true} of each SPSS is observed from the ground with a resolution that exceeds the Gaia BP/RP one by at least a factor of 4-5, and then compressed in a way that minimizes information losses. Once the SPSS spectra are smoothed, the dispersion matrix becomes a square *effective dispersion matrix*, D_e

$$S_{obs} = D_e \times S_{smooth}$$

However, D_e can still be non-diagonal or degenerate and before proceeding we must find the criteria to build the best possible D_e with the data in hand.

2.5. The ideal SPSS set

One reason why the dispersion matrix is non-diagonal, is that the SPSS adopted set can *never* be an orthogonal set of independent calibrators: stars are all similar to each other, they have all a black-body like continuum with some features (absorption and emission lines or bands). As a result, if a dispersion matrix is built with a particular set of SPSS, such as white dwarfs and hot subdwarfs (the ideal calibrators in the classic spectroscopic observations), it will be able to calibrate properly only objects with similar spectra, i.e., relatively smooth, with some absorption lines in the blue part of the spectrum.

An example of the above case is shown in Figure 7, where two different dispersion matrices are used to calibrate the same set of simulated Gaia observations. In the first

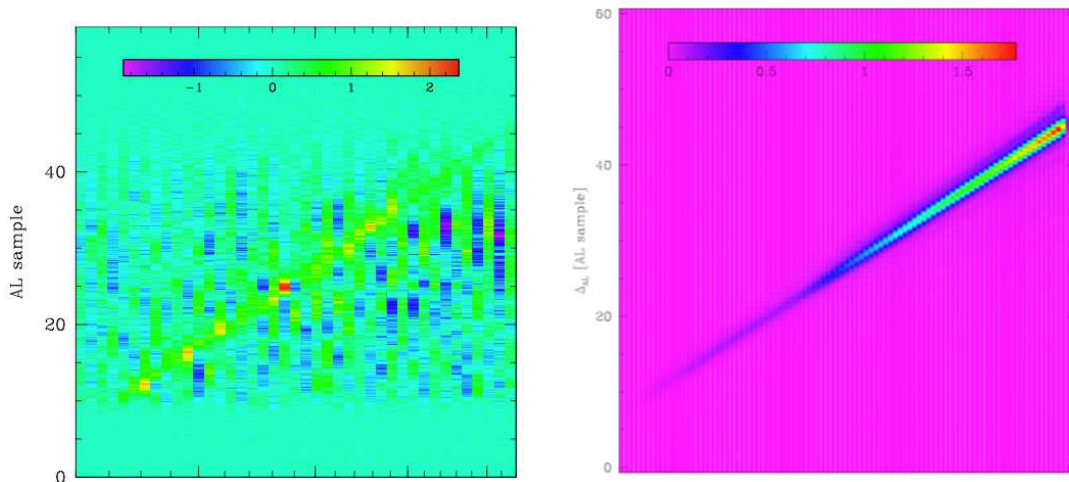


Figure 8: Left: example of a degenerate dispersion matrix, D_e (which is square, see text), where the diagonal is drowned into noise-like patterns due to the degenerate (non independent) set of SPSS used to construct it. Right: an example of a diagonal dispersion matrix, obtained with an appropriate SPSS set and with the use of a nominal dispersion matrix to further reduce degeneracy (see text).©ESA

case (left panel of Figure 7), a dispersion matrix is built using only white dwarfs and hot subdwarfs, with a minority of solar type stars, and it can clearly be seen that red stars with deep absorption bands are calibrated with an *error* of 0.15 mag at least, failing the specified requirements. In the second case (right panel of Figure 7), a small number (10) of red stars with deep absorption bands are included in the SPSS set used to build a second dispersion matrix. The second dispersion matrix is able to calibrate all red stars with absorption features to better than 1%, exceeding the requirements.

This example shows the importance of spectral features in the SPSS set used in construction of the dispersion matrix. Hot stars have prominent absorption lines in the blue, but no features in the red. The addition of a few red stars with absorption bands “trains” the matrix in the calibration of stars with features in the red (effectively reducing degeneracy). Similarly, problems are encountered in the calibration of emission line objects (peculiar hot stars and quasars, for example). But it is quite difficult to include these objects into the SPSS set since they are often variable.

Even if several types of objects are included when determining the dispersion matrix, other effects can have a large impact on the degeneracy, such as edge effects. For these reasons, the accurate choice of the SPSS set is crucial, but does not solve the problem of degeneracy once and for all.

2.6. Nominal dispersion matrix

To further reduce degeneracy of the effective dispersion matrix D_e , we can use other constraints such as the fact that we know most aspects of the instrument from pre-launch characterization. These include the quantum efficiency of the CCDs, the optical layout and transmissivity, the nominal LSF at various positions along the focal plane and at different wavelengths, the nominal dispersion function and its variation along the focal plane. The slow change of these with time can also be monitored to a certain extent, and included in the modelization.

We can therefore separate the dispersion matrix in a part that is theoretically modeled based on pre-launch instrument description and on its (partially reconstructed) variation with time, which we call D_n or *nominal dispersion matrix*, and in a part that is completely

unknown, which can be considered as a correction matrix K , made of the residual corrections after the nominal model is taken into account (Montegriffo et al. 2010)

$$D_e = K \times D_n$$

The nominal matrix will be clean: diagonal and non-degenerate (see Figure 8). The correction matrix will be partially degenerate, but all signal that lies far away from the diagonal can be safely considered spurious (the system varies in a continuous way, the corrections must be “small” compared to the nominal system), and the part of the correction matrix close to its diagonal can be easily modeled.

To summarize all the previously defined steps, once an appropriate SPSS set is chosen, the calibration model becomes

$$S_{obs} = D_e \times S_{smooth} = K \times D_n \times S_{smooth}$$

and the matrices involved can be easily inverted to calibrate all Gaia observations since they are all square and (almost completely) diagonal.

2.7. Integrated magnitudes

A classical approach can be adopted for the absolute flux calibration of integrated M_G , M_{BP} , and M_{RP} magnitudes (Ragaini et al., 2009a,b) in the form

$$M = m + ZP$$

where M is the calibrated magnitude, m the internally calibrated one observed by Gaia, and ZP is the required zero-point. No significant color term appears necessary.

However, if we consider that an integrated magnitude M is the convolution of the spectral distribution S_{true} and the effective passband B , we can calibrate integrated magnitudes with the same approach adopted for BP/RP spectra, with a much more homogeneous procedure from the point of view of pipeline code writing

$$M = S_{true} \times B$$

Since generally the passband B is sampled differently than the SPSS flux table S_{true} , we must apply smoothers to one or both S_{true} and B . Similarly to the case of BP/RP spectra, we can split B into two components

$$B = K' \times B_n$$

where K' is a correction vector, made of the actual residuals to a theoretically known – or *nominal* – effective passband B_n , known before launch and slowly varying with time due to several causes, the most important one being the CCDs quantum efficiency decreased due to radiation damage. With this kind of treatment, the problem becomes a simple least square fitting problem to derive the unknown K' vector (Ragaini et al., 2010, in preparation).

2.8. RVS calibration

The possibility of calibrating in flux the RVS spectra has been so far considered a secondary problem, since both radial velocities and astrophysical parameters can be derived without the need of an absolute flux scale attached to the spectra. A preliminary set of considerations (Trager, 2010) shows that in principle the SPSS grid for the calibration of Gaia G-band and BP/RP data, that is presently under construction, should be sufficiently sampled to ensure a flux calibration of RVS spectra as well. We expect the topic to be further explored by CU6 (Spectroscopic processing) in the near future, but we will not consider RVS spectra flux calibration in this paper.

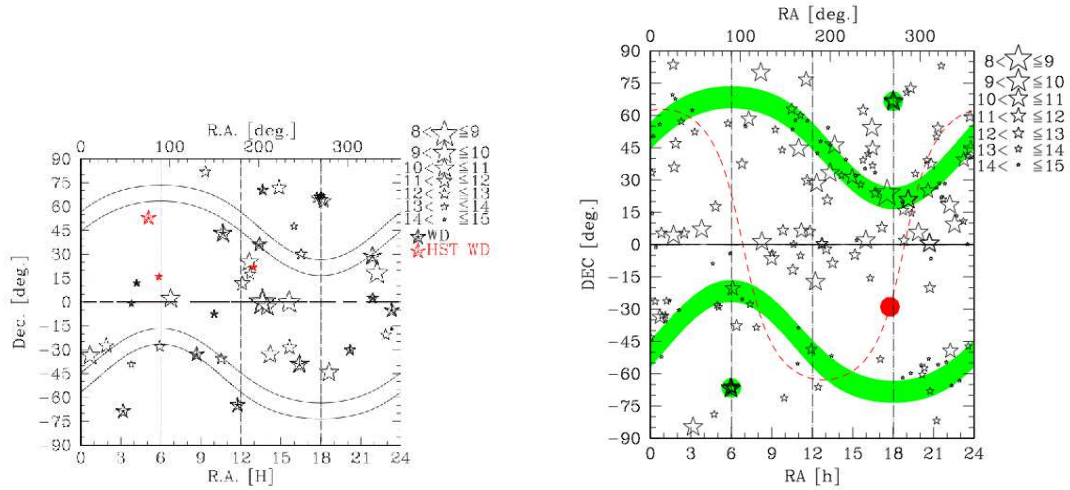


Figure 9: The Ra/Dec distribution of Primary (left) and Secondary SPSS candidates (right). The three Pillars are marked in red in the left panel, while the targets close to the ecliptic poles are marked in green in the right panel. The size of symbols is inversely proportional to the SPSS magnitude. The two stripes at ± 45 deg from the Ecliptic Poles are marked in both panels. ©ESA

3. The Gaia grid of spectrophotometric standard stars

From the above discussion, it is clear that the Gaia SPSS grid has to be chosen with great care. The Gaia SPSS, or better their reference flux tables (corresponding to S_{true} in the previous Sections) should conform to the following general requirements (van Leeuwen et al. 2010):

- Resolution $R=\lambda/\delta\lambda \simeq 1000$, i.e., they should oversample the Gaia BP/RP resolution by a factor of 4–5 at least;
- Wavelength coverage: 330–1050 nm;
- Typical uncertainty on the absolute flux scale, with respect to the assumed calibration of Vega, of a few percent, excluding small troubled areas in the spectral range (telluric bands residuals, extreme red and blue edges), where it can be somewhat worse.

The total number of SPSS in the Gaia grid should be of the order of 200–300 stars, including a variety of spectral types. Clearly, no such large and homogeneous dataset exists in the literature yet⁵. It is therefore necessary to build the Gaia SPSS grid with new, dedicated observations. We describe the characteristics of the Gaia SPSS and of the dedicated observing campaigns in the following Sections.

3.1. SPSS Candidates

We have followed a two steps approach (Bellazzini et al. 2007) that firstly creates a set of *Primary SPSS*, i.e., well known SPSS that are calibrated on the three *Pillars* of the CALSPEC⁶ set, described in Bohlin et al. (1995,2007), and tied to the Vega flux calibration

⁵The CALSPEC database (Bohlin, 2007) is not large enough for our purpose, especially considering the strict criteria described below. Its extension to more than 100 SPSS is eagerly awaited, but still not available to the public.

⁶<http://www.stsci.edu/hst/observatory/cdbs/calspec.html>

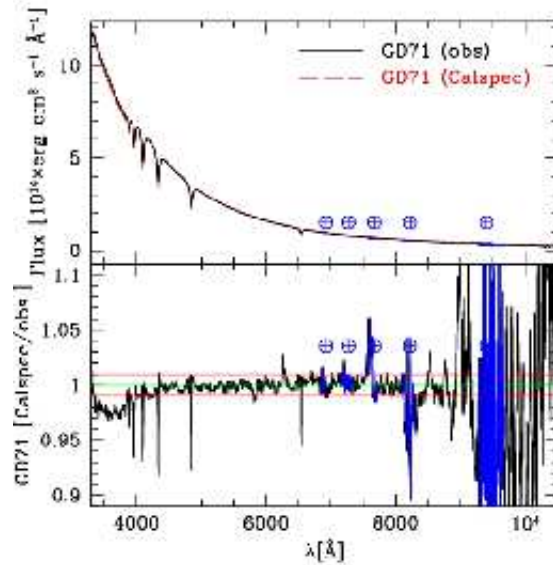


Figure 10: The preliminary reductions (no telluric correction, only TNG observations, library extinction curve, and so on) of star GD 71 (top panel) are compared with the CALSPEC spectrum (bottom panel). Prominent telluric features are marked in both panels. Except for the spectral edges – which will need to be reconstructed with the use of models – the main body of the spectrum is always close to the CALSPEC one within 1% or better. ©ESA

by Bohlin & Gilliland (2004) and Bohlin et al. (2007). An example of the kind of spectra obtained for Pillar GD 71 (with DoLoRes@TNG) is shown on Figure 10. The Primary SPSS will constitute the ground-based calibrators of the actual Gaia grid, and need to conform to the following requirements (van Leeuwen 2010):

- Primary SPSS have spectra as featureless as possible;
- Primary SPSS shall be validated against variability;
- Primary SPSS have already well known SEDs;
- The magnitude of each Primary SPSS grants a resulting $S/N \simeq 100$ per pixel over most of the wavelength range when observed from the ground with 2m class telescopes;
- The location of Primary SPSS is in non crowded areas of the sky;
- Primary SPSS cover a range of RA and Dec to ensure all-year-round ground based observations from both hemispheres.

The Primary SPSS candidates set is described in more detail in Altavilla et al. (2008), and some of the most important sources for Primary candidates are the CALSPEC grid, Oke (1990), Hamuy et al. (1992,1994), Stritzinger et al. (2005) and others. The actual Gaia SPSS grid, or *Secondary SPSS*, conforms to a different set of requirements (van Leeuwen 2010):

- Secondary SPSS have spectra as featureless as possible (but see below for exceptions);
- Secondary SPSS shall be validated against variability;

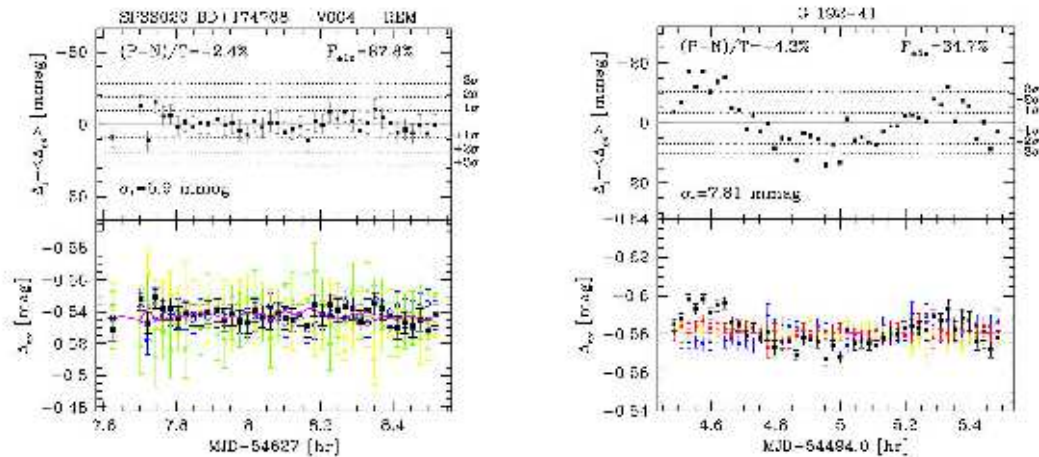


Figure 11: Left: example of a short-term variability curve for a constant SPSS candidate. Right: example of a short-term variability curve for a variable SPSS candidate. ©ESA

- The magnitude and sky location (i.e., number of useful, clean transits, see Carrasco et al. 2006, 2007) of Secondary SPSS grants a resulting $S/N \approx 100$ per sample over most of the wavelength range when observed by Gaia (end of mission);
- Secondary SPSS cover a range of spectral types and spectral shapes, as needed to ensure the best possible calibration of all kinds of objects observed by Gaia.

As already mentioned, Secondary SPSS will be mostly hot and featureless stars but will include a small number of selected spectral types, to ensure that the calibration model can work on all objects types. More details on Secondary SPSS can be found in Altavilla et al. (2010), including a long list of literature catalogues and online databases from which the candidates are extracted. Clearly, all the Primary SPSS that, at the end of the data reductions, will satisfy also the criteria for Secondary SPSS, will be included in the Gaia SPSS grid.

Additional, special members of the Secondary SPSS candidates are: (1) a few selected SPSS around the Ecliptic Poles, two regions of the sky that will be repeatedly observed by Gaia, in the first two weeks after reaching its orbit in L2, for calibration purposes; (2) a few M stars with deep absorption features in the red; (3) a few SDSS stars that have been observed in SEGUE sample (Yanny et al., 2009), since the SEGUE sample has the potential of being extremely useful in the Gaia flux calibration (Bellazzini et al. 2010), both internal (relative) and external (absolute); (4) a few well known SPSS that are among the targets of the ACCESS mission (Kayser et al., 2010), dedicated to the absolute flux measurement of a few stars besides Vega.

3.2. Observation strategy and campaigns

A basic consideration when starting the observations of such a large campaign, is that the traditional spectrophotometry techniques require too much observing time: each SPSS should be spectroscopically observed in perfectly photometric conditions, ideally more than once. No TAC (Time Allocation Committee) would grant such a large amount of observing time to a proposal that does not contain any cutting edge science in it.

We therefore chose (Bellazzini et al. 2007) to split the problem into two parts: (1) spectra are taken in good sky conditions, but not necessarily perfectly photometric; they are

calibrated with the help of a *Pillar* or *Primary SPSS* thus recovering the correct spectral *shape*; (2) absolute photometry in the B, V, and R (sometimes I) Johnson-Cousins bands is taken in photometric sky conditions and used to fix the spectral *zero-point* by means of synthetic photometry. This is motivated by the fact that absolute photometric night points are faster to obtain than spectra. A subset of SPSS candidates will be spectroscopically observed in photometric sky conditions, to check the whole procedure.

Besides the *Main Campaign* just described, it is necessary to monitor candidate SPSS for constancy (*Auxiliary Campaign*), since very few of them have systematically been monitored in the literature, and there are illustrious examples of stars that showed unexpected variability (Landolt & Uomoto, 2007). An example of a different kind of problem, that could greatly benefit from good quality dedicated imaging, is star HZ 43. It was initially chosen by Bohlin et al. (1995) to be one of the Pillars, and later rejected because of an optical companion lying 3" away, only visible in the V band, that made it useless as an SPSS from the ground.

Most of our SPSS candidates are WD close to the instability strip, and sometimes have poorly known magnitudes, so it is necessary to monitor them for short-term variability on 1–2 h (Figure 11). Binary systems are frequent and can be found at all spectral types, so we also monitor all our candidates for long-term variability (3 yrs) collecting approximately 4 night points per year. These two monitoring campaigns rely on relative photometry (using stars in the field of view) to derive variability curves. An SPSS candidate is considered constant if it does not vary with an amplitude larger than a few mmag.

The facilities that are being used for the two observing campaigns are (Federici et al., 2007, Altavilla et al. 2010):

- EFOSC@NTT, La Silla, Chile (primarily *Main campaign*);
- ROSS@REM, La Silla, Chile (primarily *Auxiliary campaign*);
- LARUCA@1.5m, San Pedro Martir, Mexico (primarily *Auxiliary campaign* and absolute photometry);
- BFOSC@Cassini, Loiano, Italy (primarily *Auxiliary campaign*);
- CAFOS@2.2m, Calar Alto, Spain (primarily *Main campaign*);
- DoLoRes@TNG, La Palma, Spain (primarily *Main campaign*);

Observations started in the second half of 2006, comprising more than 35 accepted proposals. We have been awarded a total of 230 observing nights approximately, at the rate of 33 per semester. More than 50% of this time resulted in at least partially useful data. Given the large number of facilities involved, and of different observers, it has become necessary to establish strict observing protocols (Pancino et al. 2008,2009). The campaigns are now more than 50% complete, with the spectroscopy observations 75% complete, and we expect to complete all our observing campaigns around 2013.

3.3. Data reduction and analysis

The large amount of data collected needs to be reduced and analysed with the maximum possible precision and homogeneity. An initial set of data is collected for each CCD/instrument/telescope combination and an “Instrument Familiarization Plan” (IFP) is conducted, to derive shutter times, linearity, calibration frames and lamps stability, photometric distortions, 2nd order contamination of spectra (Figure 12), and so on. This plan is now almost complete, and the protocols are presently being finalized and written.

The data reduction is regulated by strict data reduction protocols, that are presently being finalized. While the data reduction methods are fairly standard, care must be taken

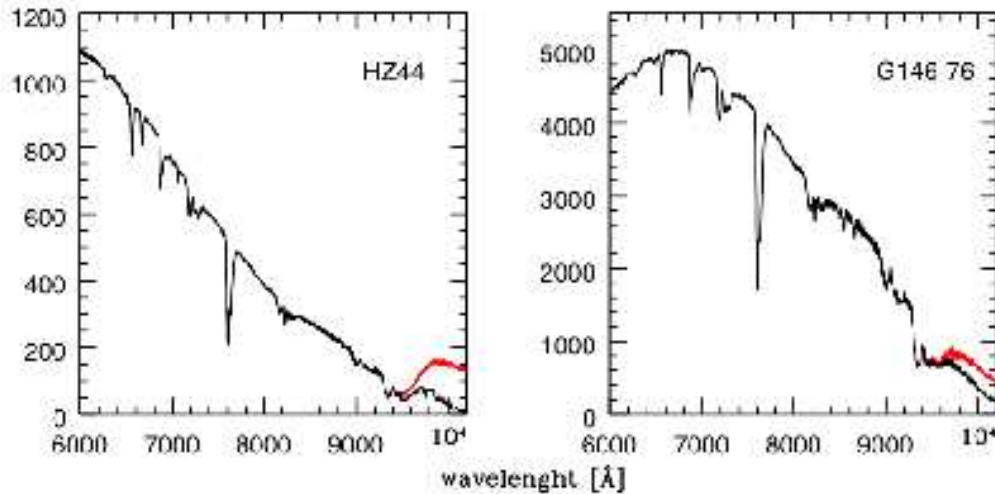


Figure 12: Example of the 2^{nd} order contamination in the DoLoRes grism LR-R, and of its correction for stars HZ 44 and G 146–76. The solid black curves are the corrected spectra while the red curves are the contaminating light coming from the 2^{nd} order dispersed blue light. ©ESA

in considering the characteristics of each instrument as determined during the IFP, to extract the highest possible quality from each instrument. Semi-automatic quality check (QC) criteria are defined for each kind of observation (minimum/maximum S/N, seeing and roundness requirements of images, presence of bad columns, companions, and so on). Only frames that pass the QC are reduced. For imaging, we term “data reduction” the removal of the instrument characteristics (dark, bias, flat-field, fringing), QC, and the measurement of aperture photometry with SExtractor (Bertin & Arnouts, 1996). The data products are 2D reduced images and aperture magnitude catalogues. For spectroscopy, we term “data reduction” the removal of instrumental features (dark, bias, flat-field, illumination correction, wavelength calibration, 2^{nd} order contamination correction, relative flux calibration, telluric features removal), followed by QC and spectra extraction. The data products are 2D reduced frames, 1D extracted and wavelength calibrated spectra, 1D flux calibrated spectra, 1D telluric absorption corrected spectra.

The data reduction procedures are well advanced for photometry (almost half of the data reduced) and are just started for spectra (10% of the data reduced) at the moment of writing.

The data analysis is presently in the design and testing phases. The study of short-term variability curves is proceeding (10% of the data analysed, see Figure 11). Absolute photometry and relative spectroscopy procedures are being refined: for example, preliminary end-to-end reduction of photometric imaging nights have been performed for TNG and NTT observations, to allow us to identify those nights that were actually photometric and did not need to be repeated. Preliminary extinction curves have been determined for TNG and CAHA spectroscopic observations, allowing us to see that extinction varies in a grey manner (within a few percent) even in the case of some Calima (desert dust) in the sky in La Palma.

The final data products for the *Auxiliary campaign* will be relative magnitudes and lightcurves for all the monitored candidate SPSS; for the *Main campaign*, absolute magnitudes and errors will be released together with their uncertainties and flux tables (Fig-

#	Run ID	Telescope	Instrument	Date obs.
1	P001	Cassini	BP/RS	19/02/06
2	P001	Cassini	BP/RS	21/02/06
3	P002	Cassini	BP/RS	22/02/06
4	P005	Cassini	BP/RS	05/02/07
5	P003	CAFA2.2	CAPOS	30/03/07
6	P003	CAFA2.2	CAPOS	31/03/07
7	P003	CAFA2.2	CAPOS	01/04/07
8	P003	CAFA2.2	CAPOS	02/04/07
9	P003	CAFA2.2	CAPOS	03/04/07
10	P003	CAFA2.2	CAPOS	04/04/07
11	P003	CAFA2.2	CAPOS	06/04/07
12	P004	TNG	DOLores	20/03/07
13	P001	TNG	DOLores	21/03/07
14	P004	TNG	DOLores	22/03/07
15	P003	CAFA2.2	CAPOS	28/03/07
16	P003	CAFA2.2	CAPOS	29/03/07
17	P003	CAFA2.2	CAPOS	30/03/07
18	P003	CAFA2.2	CAPOS	06/04/07
19	P003	CAFA2.2	CAPOS	07/04/07
20	P003	CAFA2.2	CAPOS	08/04/07

Figure 13: The simple browsing interface of the Wiki-Bo local SPSS archive. This snapshot refers to the *raw data archive*, a similar web page exists for data products. ©ESA

ure 10) in the form $(\lambda(\text{nm}), F_\lambda(\text{photons s}^{-1} \text{ m}^{-2} \text{ nm}^{-1}))$. Possibly, also other intermediate data products will be released (see above).

3.4. Data availability

All the data coming from ground based observations of SPSS, along with the collected literature information and measurements, are stored in the CU5-DU13 local Wiki pages in Bologna (Wiki-Bo)⁷. Wiki-Bo contains also all our technical documentation, internal reports, observation status and data products, along with literature references and sources, observing proposals and all the like. The raw and reduced data products are stored in a local archive⁸ for internal purposes (Figure 13).

In the future, when CU9 will be started (Catalogue production and access) it is foreseen that all the ground-based data that are used for the calibration of Gaia data (radial velocity standards, SPSS, spectral libraries, Ecliptic pole observations, observations of Gaia itself from the ground, and so on) will be published as well, although no decision on the format and type of data products has been taken yet.

4. Conclusions

The Gaia mission and its data reduction is a challenging enterprise, carried on by ESA and the European scientific community. As an example of the DPAC (Data Processing and Analysis Consortium) tasks, I have briefly summarized the problem of the external (absolute) flux calibration of (spectro)photometric Gaia data, and more specifically of the BP/RP low resolution spectra and the integrated G-band and BP/RP magnitudes. An innovative calibration model is presently under study and testing, and a large ($\simeq 200 - 300$) grid of SPSS with 1–3% flux calibration with respect to Vega is being built from multi-site ground-based observations.

But once the Gaia data will become available, a greater challenge will have to be faced: the impact in almost all fields of astrophysics require that the scientific community (and not only the European one) be adequately prepared to extract the most scientific output from

⁷<http://yoda.bo.astro.it/wiki>, guest username and password can be obtained from E. Pancino.

⁸<http://spss.bo.astro.it>, guest username and password can be obtained from E. Pancino.

the data. The training of a new generation of scientists, and the collection of complementary data, necessary to answer key questions when combined with Gaia data, should start now. The challenge requires that large groups of scientists get efficiently organized and ready to collaborate on large and comprehensive datasets.

References

- Altavilla, G., Bellazzini, M., Pancino, E., Bragaglia, A., Cacciari, C., Diolaiti, E., Federici, L., Montegriffo, P., Rossetti, E., 2008, “*Primary standards for the establishment of the Gaia grid of SPSS. Selection criteria and a list of candidates*”, Gaia technical report GAIA-C5-TN-OABO-GA-001
- Altavilla, G., Bragaglia, Pancino, E., Bellazzini, M., A., Cacciari, C., Federici, L., Ragaini, S., 2010, “*Secondary standards for the establishment of the Gaia grid of SPSS. Selection criteria and a list of candidates*”, Gaia technical report GAIA-C5-TN-OABO-GA-003
- Bellazzini, M., Bragaglia, A., Federici, L., Diolaiti, E., Cacciari, C., Pancino, E., 2006, “*Absolute calibration of Gaia photometric data. I. General considerations and requirements*”, Gaia technical report GAIA-C5-TN-OABO-MBZ-001
- Bellazzini, M., Altavilla, G., Cacciari, C., 2010, “*Notes on the possible use of SEGUE spectrophotometry for the absolute photometric calibration of Gaia*”, Gaia technical report GAIA-C5-TN-OABO-MBZ-002
- Bertin, E., & Arnouts, S. 1996, A&AS, 117, 393
- Bessell, M. S. 1999, PASP, 111, 1426
- Bohlin, R. C., Colina, L., & Finley, D. S. 1995, AJ, 110, 1316
- Bohlin, R. C. 2007, PASP, The Future of Photometric, Spectrophotometric and Polarimetric Standardization, 364, 315
- Carrasco, J. M., Jordi, C., Figueras, F., Anglada-Escudé, G., 2006, “*Towards a selection of standard stars for absolute flux calibration. Signal-to-nois ratios for BP/RP spectra and crowding due to FoV overlapping*”, Gaia technical report GAIA-C5-TN-UB-JMC-002
- Carrasco, J. M., Jordi, C., Lopez-Marti, B., Figueras, F., Anglada-Escudé, G., Amores, E. B., 2007, “*Revolving phase effect to FoV overlapping and its application to Primary SPSS*”, Gaia technical report GAIA-C5-TN-UB-JMC-002
- Carrasco, J. M. et al., 2010, in preparation, “*Design of the experiment to test BP/RP full forwarding model*”, Gaia technical report GAIA-C5-TN-UB-JMC-011
- Hamuy, M., Suntzeff, N. B., Heathcote, S. R., Walker, A. R., Gigoux, P., & Phillips, M. M. 1994, PASP, 106, 566
- Hamuy, M., Walker, A. R., Suntzeff, N. B., Gigoux, P., Heathcote, S. R., & Phillips, M. M. 1992, PASP, 104, 533
- Kaiser, M. E., et al. 2010, arXiv:1001.3925
- Landolt, A. U., & Uomoto, A. K. 2007, AJ, 133, 768
- Montegriffo, P., & Bellazzini, M. 2009a, “*A model for the absolute photometric calibration of Gaia BP and RP spectra. III. A full in-flight calibration of the model parameters*”, Gaia technical report GAIA-C5-TN-OABO-PMN-003
- Montegriffo, P., & Bellazzini, M. 2009b, “*Quantitative estimate of the uncertainty on the wavelength calibration as derived from the absolute calibration process*”, Gaia technical report GAIA-C5-TN-OABO-PMN-004
- Montegriffo, P., et al., 2010, in preparation “*Planning an experiment on source and instrument update XP processing*”, Gaia technical report GAIA-C5-TN-OABO-PMN-005

- Oke, J. B. 1990, AJ, 99, 1621
- Perryman, M. A. C., Lindegren, L., & Turon, C. 1997, Hipparcos - Venice '97, 402, 743
- Pancino, E., Altavilla, G., Bellazzini, M., Marinoni, S., Bragaglia, A., Federici, L., Cacciari, C., 2008, “*Protocol for ground based observations of SPSS. I. Instrument familiarization tests*”, Gaia technical report GAIA-C5-TN-OABO-EP-001
- Pancino, E., Altavilla, G., Carrasco, J. M., M, Monguio, Marinoni, S., Rossetti, E., Bellazzini, M., Bragaglia, A., Federici, L., Schuster, W., 2009, “*Protocol for ground based observations of SPSS. II. Variability searches and absolute photometry campaigns*”, Gaia technical report GAIA-C5-TN-OABO-EP-003
- Ragaini, S., Bellazzini, M., Montegriffo, P., Cacciari, C., 2009a, “*Absolute calibration of G and integrated BP and RP fluxes*”, Gaia technical report GAIA-C5-TN-OABO-SR-001
- Ragaini, S., Montegriffo, P., Bellazzini, M., Cacciari, C., 2009b, “*Absolute calibration of G and integrated BP and RP fluxes: test and limits of a simple model*”, Gaia technical report GAIA-C5-TN-OABO-SR-002
- Ragaini, S., et al., 2010, in preparation “*Absolute calibration of G and integrated BP and RP fluxes: a new model*”, Gaia technical report GAIA-C5-TN-OABO-SR-003
- Stritzinger, M., Suntzeff, N. B., Hamuy, M., Challis, P., Demarco, R., Germany, L., & Soderberg, A. M. 2005, PASP, 117, 810
- Trager, S., 2010, “*Spectrophotometric calibration of RVS using CU5-DU13 flux calibration tables*”, Gaia technical report GAIA-C5-TN-UG-ST-002
- van Leeuwen, F. & the CU5 DU managers, 2010, “*CU5 software requirements specifications*”, Gaia technical report GAIA-C5-SP-IOA-FVL-014
- Yanny, B., et al. 2009, AJ, 137, 4377